

Carbohydrate carbonyl mobility—the key process in the formation of α -dicarbonyl intermediates

Oliver Reihl, Thorsten M. Rothenbacher, Markus O. Lederer and Wolfgang Schwack*

Institut für Lebensmittelchemie (170), Universität Hohenheim, Garbenstr. 28, D70593 Stuttgart, Germany

Received 5 January 2004; received in revised form 3 March 2004; accepted 27 March 2004

Available online 10 May 2004

Abstract—Covalently cross-linked proteins are among the major modifications caused by the advanced Maillard reaction. In the present study, the formation pathway of the dideoxyosone *N*⁶-(2,3-dihydroxy-5,6-dioxohexyl)-L-lysine is shown. To elucidate the formation of this glucose-derived dideoxyosone D-lactose (O- β -D-galp-(1 \rightarrow 4)-D-glcp) and D-glucose-6-phosphate were incubated with lysine in the presence of the trapping reagent *o*-phenylenediamine (OPD). Synthesis and unequivocal structural characterization were reported for the quinoxalines of the dideoxyosones *N*⁶-(5,6-dihydroxy-2,3-dioxohexyl)-L-lysine and *N*⁶-(2,3-dihydroxy-4,5-dioxohexyl)-L-lysine, respectively. Additionally, dicarbonyl compounds derived from D-erythrose, D-glycero-D-mannoheptose, and D-gluco-L-taloctose were synthesized and structurally characterized.

© 2004 Elsevier Ltd. All rights reserved.

Keywords: Maillard reaction; Quinoxaline; Dideoxyosone; *o*-Phenylenediamine (OPD); Advanced glycation end product (AGE)

1. Introduction

The Maillard reaction or ‘nonenzymatic browning’ is a complex series of reactions between reducing carbohydrates and lysine side chains or N-terminal amino groups of proteins. In the first step of this process, rather labile Schiff bases are formed, which as a rule rearrange to the more stable Amadori products. In complex reaction pathways via dicarbonyl intermediates the Amadori compounds are slowly degraded to a plethora of compounds^{1,2} subsumed summarily under the term ‘advanced glycation end products’ (AGEs). This overall reaction sequences proceed both in vivo and in foods. Most AGEs are formed from aminoketoses via highly reactive dicarbonyl intermediates such as **1–8** (Fig. 1).^{1,3–10} In long-living connective tissue and matrix components, AGEs accumulate with age and are generated to a greater extent in diabetes.¹¹ AGEs can activate cellular receptors^{12–14} and contribute to the pathophysiology associated with aging in general as well

as with long-term complications of diabetes, atherosclerosis, and Alzheimer’s disease.^{1,15–18} To gain a better understanding of the impact of the Maillard reaction on these processes and develop effective therapeutic methods against AGE accumulation in tissues, it is necessary

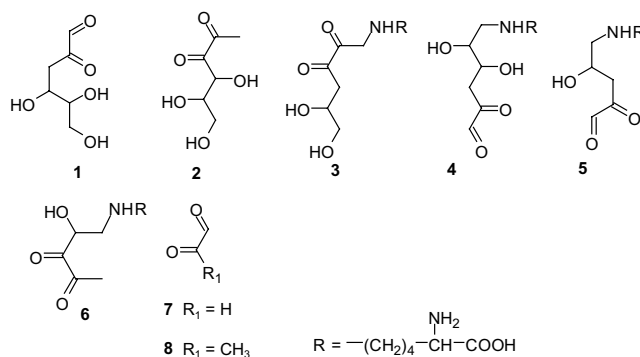


Figure 1. Important dicarbonyl intermediates in the formation of cross-links: 3-deoxyhexos-2-ulose (**1**), 1-deoxyhexo-2,3-diulose (**2**), *N*⁶-(5,6-dihydroxy-2,3-dioxohexyl)-L-lysine (**3**), *N*⁶-(2,3-dihydroxy-5,6-dioxohexyl)-L-lysine (**4**), *N*⁶-(2-hydroxy-4,5-dioxopentyl)-L-lysine (**5**), *N*⁶-(2-hydroxy-3,4-dioxopentyl)-L-lysine (**6**), glyoxal (GO **7**), and methylglyoxal (MGO **8**).

* Corresponding author. Tel.: +49-711-4593979; fax: +49-711-45940-96; e-mail: wschwack@uni-hohenheim.de

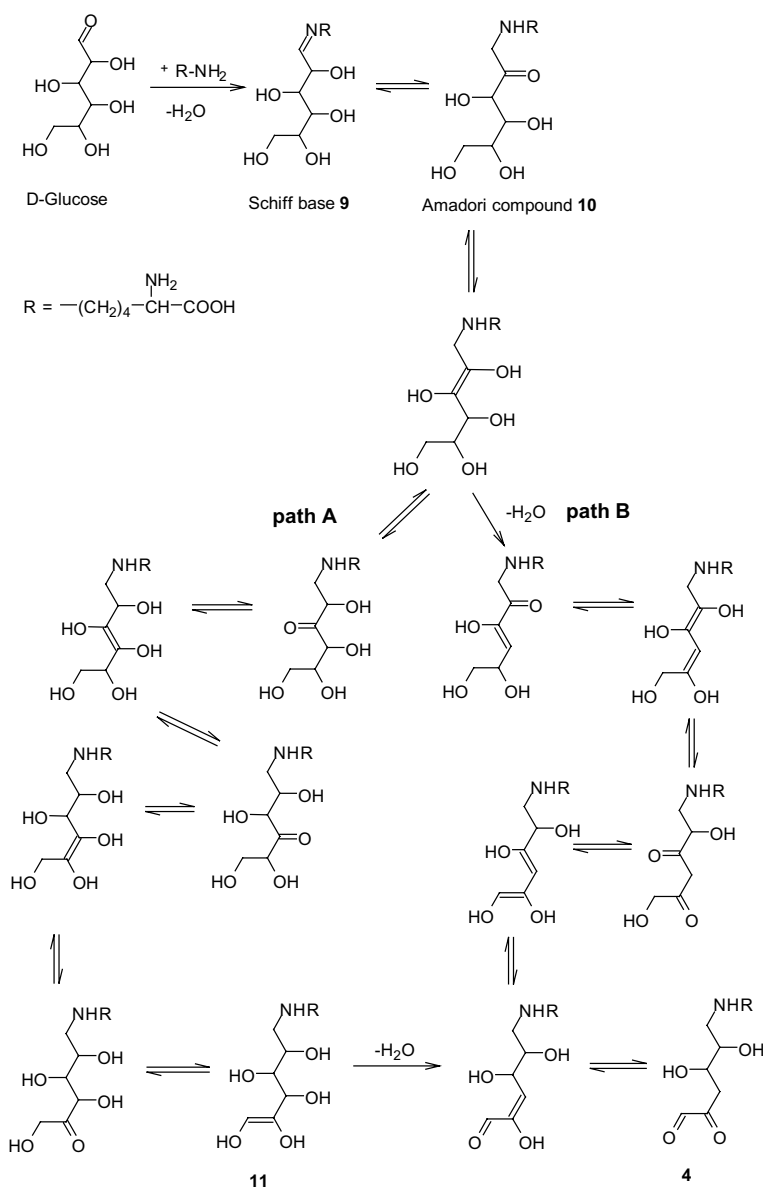
to identify the formation pathways of the major Maillard protein cross-links.^{15,16,19–22}

Recently, Biemel et al.¹⁰ identified the dideoxyosones *N*⁶-(2,3-dihydroxy-5,6-dioxohexyl)-L-lysine (**4**), *N*⁶-(2-hydroxy-4,5-dioxopentyl)-L-lysine (**5**), and *N*⁶-(2-hydroxy-3,4-dioxopentyl)-L-lysine (**6**, Fig. 1). In these structures, *N*^ε of the lysine moiety is directly bonded to C-1 of the original sugar. The formation of these compounds proceeds via carbonyl shifts along the carbohydrate backbone.

The dideoxyosone **4** is thus not only pivotal in the formation of the major in vivo Maillard cross-link 6-[2-[(4*S*)-4-ammonio-5-oxido-5-oxopentyl]amino-6,7-dihydroxy-6,7,8,8a-tetrahydroimidazo[4,5-*b*]azepin-4(5*H*)-yl]-L-norleucinate (glucosepane),¹⁰ but may represent

the key intermediate for numerous other Maillard products. However, the formation pathway of **4** is not understood in detail. In Scheme 1, starting from native D-glucose two plausible pathways (A and B) for the formation of **4** are presented. Path A describes the enolization along the entire carbohydrate backbone, leading to the endiol **11**, which eliminates water at C-4 and finally yields the tautomer **4**. Path B describes the water elimination in position C-4 in an early step, the enolization proceeds along the sugar backbone forming the α-dicarbonyl **4**.

We presently report on the elucidation of the formation pathway of the dideoxyosone *N*⁶-(2,3-dihydroxy-5,6-dioxohexyl)-L-lysine (**4**) as well as of the structural characterization of the quinoxalines of the dicarbonyl



Scheme 1. Proposed formation pathways for the dideoxyosone *N*⁶-(2,3-dihydroxy-5,6-dioxohexyl)-L-lysine (**4**).

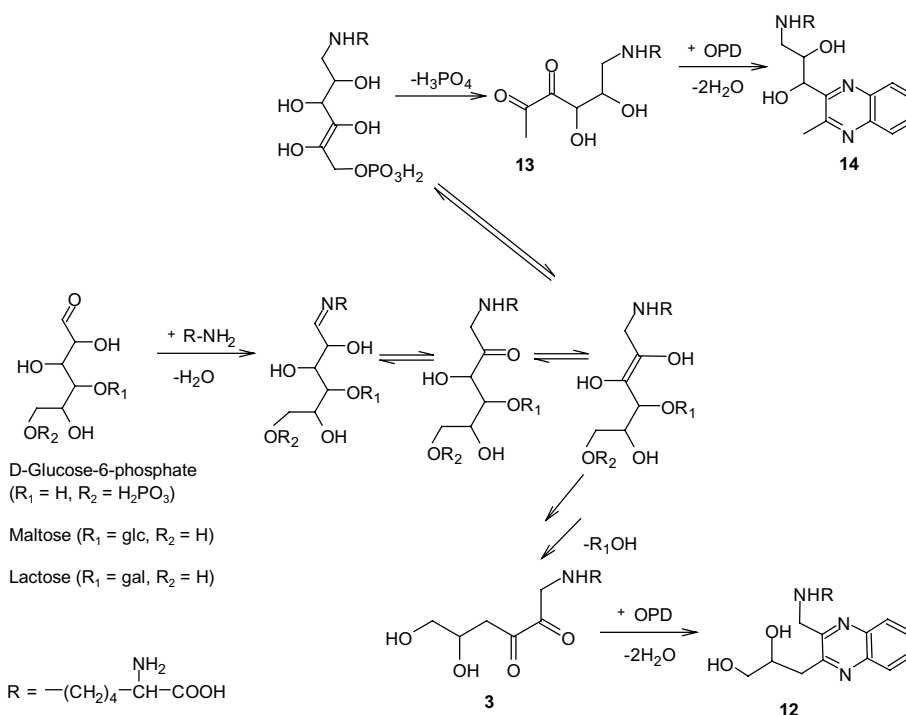
compounds N^6 -(5,6-dihydroxy-2,3-dioxohexyl)-L-lysine (**3**) and N^6 -(2,3-dihydroxy-4,5-dioxohexyl)-L-lysine (**13**). Additionally, further quinoxalines derived from D-erythrose, D-glycero-D-mannoheptose, and D-gluco-L-taloctose, respectively, were independently synthesized and the dideoxyosone structures N^6 -(2,3-dioxobutyl)-L-lysine (**15**), N^6 -(2,3,7-trihydroxy-5,6-dioxohexyl)-L-lysine (**17**), and N^6 -(2,3,7,8-tetrahydroxy-5,6-dioxooctyl)-L-lysine (**19**) unequivocally established.

2. Results and discussion

Detection of high reactive α -dicarbonyls, for example, **4**, in the free form is very difficult to be performed. Therefore, isolation of such compounds is mostly carried out after transformation into stable derivatives. The most used trapping reagent for α -dicarbonyls is *o*-phenylenediamine (OPD), which generates stable quinoxalines and yielded with **4**, for example, N^6 -[2,3-dihydroxy-4-(2-quinoxaliny)butyl]-L-lysine (structure not shown).^{1,10} Recently, it was proven by Biemel and Lederer that the formation of **4** was not significantly catalyzed by OPD, which acts only as a trapping reagent.²³ Another well-known trapping reagent for α -dicarbonyl compounds is aminoguanidine, which results in the formation of triazine derivatives.

To prove the formation pathway of **4**, different hexoses such as D-galactose, D-glucose, and D-mannose

were incubated with N^{α} -*t*-Boc-L-lysine and OPD in phosphate buffer (pH 7.4) at 50 °C, respectively. Aliquots were taken at regular intervals, the protective group was cleaved off in acidic medium (3 M HCl), and the mixtures were analyzed by LC-(ESI)MS. The retention time (t_R 8.3 min), UV spectra, and quasimolecular ions $[M+H]^+$ at m/z 363 of the obtained quinoxalines (chromatograms not shown) were identical to those reported previously for the glucose-derived quinoxaline.¹⁰ The results indicate that all hexoses yield the same dideoxyosone **4** (Scheme 1). In order to determine the influence of a substituent on the location of the diketone unit, glycosidic (1 \rightarrow 4) linked disaccharides such as D-lactose (*O*- β -D-galp-(1 \rightarrow 4)-D-glcp) and D-maltose (*O*- α -D-glcp-(1 \rightarrow 4)-D-glcp) were also incubated with N^{α} -*t*-Boc-L-lysine in the presence of OPD. Aliquots of the crude reaction mixtures were taken and, after cleavage (3 M HCl) of the protective group, analyzed by LC-(ESI)MS. Quinoxalines with the same quasimolecular ions $[M+H]^+$ at m/z 363 and the same UV spectra, but different in retention time (t_R 5.6 min, chromatograms not shown) as compared to the hexose-derived quinoxalines were detected. To elucidate the structure of this unknown quinoxaline, D-lactose was incubated in higher amounts with N^{α} -*t*-Boc-L-lysine and OPD in phosphate buffer (pH 7.4) at 60 °C for 3 days. The compound with the quasimolecular ion $[M+H]^+$ at m/z 463 (*t*-Boc-**12**, Scheme 2) was isolated, the protective group was hydrolyzed, and the product was purified by



Scheme 2. Formation pathway for the dideoxyosones N^6 -(5,6-dihydroxy-2,3-dioxohexyl)-L-lysine (**3**) and N^6 -(2,3-dihydroxy-4,5-dioxohexyl)-L-lysine (**13**), derived from the (1 \rightarrow 4) disaccharides lactose/maltose and glucose-6-phosphate, respectively. The dideoxyosones were trapped as their respective quinoxalines **12** and **14**.

preparative HPLC. Accurate mass determination gave $[M+H]^+$ at m/z 363.2028, corresponding to the loss of one *t*-Boc group from m/z 463 and an elemental composition of $C_{18}H_{26}N_4O_4$. The NMR data, compiled in Table 1, unequivocally prove the formation of N^6 -{[3-(2,3-dihydroxypropyl)quinoxalin-2-yl]methyl}-L-lysine (**12**). The results clearly indicate that the glycosidic bond blocks the keto–enol tautomerization along the entire carbohydrate backbone and that (1 → 4) glycosides eliminate the substituent at C-4 yielding solely the 2,3-dideoxyosone N^6 -(5,6-dihydroxy-2,3-dioxohexyl)-L-lysine (**3**, Scheme 2). The free dideoxyosone **3** has already been described during the Maillard reaction of disaccharides.^{21,24}

As an example of a carbohydrate substituted at position C-6, D-glucose-6-phosphate was reacted with N^α -*t*-Boc-L-lysine and OPD in phosphate buffer (pH 7.4) at 60 °C for 3 days. The reaction process was monitored by LC-(ESI)MS analysis and two peaks of diastereoisomers with $[M+H]^+$ at m/z 463 were detected (*t*-Boc-**14**, Scheme 2). In the crude reaction mixture two signals for the quinoxaline derivatives of 1- and 3-deoxyglucosones were also identified nearly in same quantities. The two diastereoisomers were isolated, the *t*-Boc-group was eliminated, and the products were purified by preparative HPLC. Accurate mass determination of the obtained compounds gave $[M+H]^+$ at m/z 363.2033 and established the elemental composition $C_{18}H_{26}N_4O_4$. The NMR data (Table 1) prove the formation of N^6 -[2,3-dihydroxy-3-(3-methylquinoxalin-2-yl)propyl]-L-lysine (**14**), existing as a pair of diastereoisomers **14a** and **14b**. With D-glucose-6-phosphate, the phosphate moiety was eliminated resulting in the formation of the 4,5-dideoxyosone **13**.

To validate this finding, further experiments were performed with the (1 → 6) glycosidic linked carbohydrates D-melibiose (*O*- α -D-galp-(1 → 6)-D-glcp) and D-gentiobiose (*O*- β -D-glcp-(1 → 6)-D-glcp). After incubation with N^α -*t*-Boc-L-lysine and OPD, for both experiments two signals of the diastereoisomers of *t*-Boc-**14** with the same quasimolecular ions $[M+H]^+$ at m/z 463 and the same retention time could be detected by LC-(ESI)MS (chromatograms not shown). Therefore, it must be concluded that also for the (1 → 6) glycosidic linked disaccharides melibiose and gentiobiose the substituent at C-6 was eliminated. Generally, all disaccharides and D-glucose-6-phosphate showed the same behavior. They preferentially eliminated their substituents and form the dideoxyosones **3** and **13**, respectively (Scheme 2).

Therefore it can be concluded that glycosylated (disaccharides) or phosphorylated (D-glucose-6-phosphate) hydroxyl groups prevent the keto–enol tautomerization along the carbohydrate backbone. The enolization completely along the entire sugar skeleton only proceeds in the presence of unsubstituted hydroxyl groups. These

findings support that the formation of **4**, which requires enolization from C-1 to C-6, proceeds according to path A outlined in Scheme 1.

Further experiments were performed to gain information about the carbonyl mobility in glucose homologues. On the incubation of D-erythrose, a C₄ carbohydrate, with N^α -*t*-Boc-L-lysine and OPD, the LC-(ESI)MS analysis detected one peak with $[M+H]^+$ at m/z 403 (*t*-Boc-**16**, Scheme 3a). After isolation and elimination of the *t*-Boc-group, the elemental composition of **16** was confirmed by accurate mass determination (m/z 303.1828 for $[M+H]^+$). ¹H and ¹³C NMR data (chemical shifts, δ ; coupling constants, *J*) presented in Table 1 establish the formation of N^6 -[(3-methylquinoxalin-2-yl)methyl]-L-lysine (**16**). The structural characterization of **16** confirmed N^6 -(2,3-dioxobutyl)-L-lysine (**15**, Scheme 3a) as the respective tetrose-derived dideoxyosone, showing that the formation of the 2,3-dideoxyosone **15** is preferred, whereas the expected 3,4-dideoxyosone (structure not shown) was formed only in small amounts. This phenomenon was also observed for pentose-derived dideoxyosones.¹⁰

The C₇ and C₈ carbohydrates D-glycero-D-mannoheptose and D-gluco-L-taloctose were also allowed to react with N^α -*t*-Boc-L-lysine in the presence of OPD and the reaction processes were monitored by LC-(ESI)MS analysis. In both cases, two twin peaks with $[M+H]^+$ at m/z 493 (*t*-Boc-**18**) and m/z 523 (*t*-Boc-**20**) could be observed for the first and second experiment, respectively (Scheme 3b and c). The respective compounds were isolated, purified as described, and the expected elemental compositions $C_{19}H_{29}N_4O_5$ for **18** (m/z 393.2139) and $C_{20}H_{31}N_4O_6$ for **20** (m/z 423.2232), respectively, were confirmed by accurate mass determination. NMR spectroscopic analysis (Table 2) demonstrated the formation of N^6 -{2,3-dihydroxy-4-[3-(hydroxymethyl)quinoxalin-2-yl]butyl}-L-lysine (**18**) and N^6 -{4-[3-(1,2-dihydroxyethyl)-quinoxalin-2-yl]-2,3-dihydroxy-butyl}-L-lysine (**20**). Both **18** and **20** are existing as a pair of diastereoisomers **a** and **b**. Although, the enolization reaction along the entire carbohydrate backbone should also be possible, the C₇ and C₈ carbohydrates mainly produced, after water elimination at C-4, the 5,6-dideoxyosones **17** and **19**, respectively (Scheme 3b and c). This conclusion is strongly supported by the results of experiments with D₂O as solvent. By means of LC-(ESI)MS and NMR spectroscopy it was proven that isotopomers of **19** were obtained, which represented D-C-OH units only at C-2 and C-3. This means that these stereogenic centers have undergone H/D exchange in the course of keto–enol tautomerization and that the enolization along the carbohydrate backbone does not exceed C-5. Whether these unexpected results are based on steric effects or ring structures is still an open question. Concerning the presented schemes and figures the respective sugars and

Table 1. ^1H and ^{13}C NMR spectroscopic data of **12**, **14**, and **16**^a in D_2O

	12	14a	14b	16
^1H NMR	δ (ppm) ^b			
H _A -1	4.66	3.28	3.24	
H _B -1	4.73	3.43	3.27	
H ₂ -1				4.53
H-2		4.39	4.45	
H-3		5.19	5.14	
H _A -4	3.04			
H _B -4	3.06			
H ₃ -4				2.50
H-5	4.17			
H _A -6	3.58			
H _B -6	3.68			
H ₃ -6		2.72	2.67	
H ₂ -1'	3.23	3.09	3.06	3.21
H ₂ -2'	1.79	1.73	1.69	1.78
H ₂ -3'	1.42	1.42	1.42	1.43
H ₂ -4'	1.80	1.84	1.81	1.83
H-5'	3.68	3.69	3.66	3.66
H-3''	8.02	7.90	7.82	7.84
H-4''	7.77	7.76	7.73	7.77
H-5''	7.79	7.76	7.76	7.77
H-6''	7.94	8.01	7.97	7.94
J (Hz) ^c				
$^2J_{1\text{A},1\text{B}}$	(-)16.5	(-)13.0	(-)12.8	
$^2J_{4\text{A},4\text{B}}$	(-)14.9			
$^2J_{6\text{A},6\text{B}}$	(-)11.7			
$^3J_{1\text{A},2}$		9.4	8.6	
$^3J_{1\text{B},2}$		2.9	3.7	
$^3J_{2,3}$		7.0	4.0	
$^3J_{4\text{A},5}$	8.0			
$^3J_{4\text{B},5}$	≈5.0			
$^3J_{5,6\text{A}}$	6.2			
$^3J_{5,6\text{B}}$	4.0			
$^3J_{1',2'}$	7.8	8.0	7.8	7.7
$^3J_{4',5'}$	6.4	6.0	6.1	6.3
^{13}C NMR	δ (ppm) ^b			
C-1	49.1	50.2	50.5	48.8
C-2	147.4	69.9	69.2	147.8
C-3	152.8	72.6	71.9	152.2
C-4	37.4	154.2	153.7	20.5
C-5	71.8	154.7	153.9	
C-6	65.5	22.4	22.5	
C-1''	47.8	48.3	48.4	47.7
C-2''	25.8	25.9	26.1	25.3
C-3''	22.1	22.1	22.1	22.1
C-4''	30.4	30.7	30.9	30.1
C-5''	54.9	55.4	55.5	54.6
C-6''	175.0	175.4	175.5	174.5
C-1''	140.1	140.9	140.5	140.5
C-2''	140.9	141.2	141.2	141.0

(continued on next page)

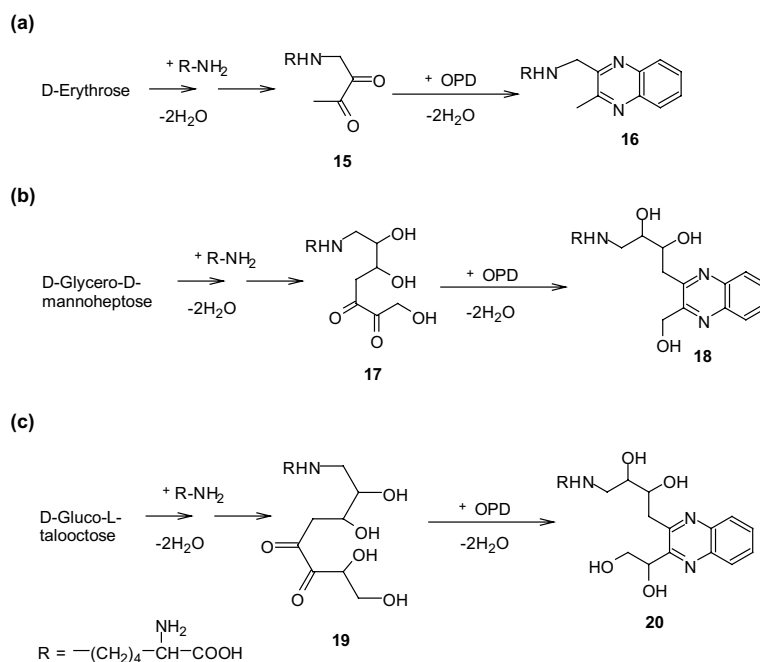
Table 1 (continued)

	12	14a	14b	16
C-3''	128.9	127.9	127.9	127.7
C-4''	131.0	132.0	132.0	131.2
C-5''	131.6	131.0	131.1	131.2
C-6''	127.8	128.9	129.1	129.3

^aThe arrows in the structural formulas indicate the characteristic carbon–proton long-range coupling connectivities from the gs-HMBC spectra. Hydrogen/carbon assignment has been validated by ¹H, ¹H-COSY, TOCSY 1D, gs-HSQC, and gs-HMBC measurements.

^b δ (ppm), chemical shift for the indicated hydrogen/carbon.

^c J (Hz), coupling constant between the indicated protons.



Scheme 3. Identification of the dideoxyosones. (a) *N*⁶-(2,3-Dioxobutyl)-L-lysine (**15**) starting from tetrose, (b) *N*⁶-(2,3,7-trihydroxy-5,6-dioxohexyl)-L-lysine (**17**) from heptose, and (c) *N*⁶-(2,3,7,8-tetrahydroxy-5,6-dioxooctyl)-L-lysine (**19**) from octose. All dideoxyosones were trapped as their respective quinoxalines **16**, **18**, and **20**.

their derivatives, for simplification, are shown in acyclic forms. But, it must be noted that both Schiff bases and Amadori products predominantly exist in the cyclic form. However, it is generally known that acyclic forms of carbohydrates represents the major reactive species.^{25,26}

In the present study, the formation pathway of the dideoxyosone *N*⁶-(2,3-dihydroxy-5,6-dioxohexyl)-L-lysine (**4**) following path A (Scheme 1) was elucidated. Starting from the Amadori product **10**, the formation proceeds via several enolization steps followed by 1,4-elimination of water at C-4 and rearrangement to **4**. Beside **4**, compounds **3** and **13** represent quantitatively significant intermediates during the degradation of 1,4-glycosidic linked disaccharides and glucose-6-phosphate, respectively. The dideoxyosones **3**, **4**, and **13** can play a major role in foodstuffs, and **4** and **13** in living systems as well. In contrast to heated foodstuffs, incubations performed at 60 °C will be, of course, somewhat different in kinetics and amounts under in vivo condi-

tions. Biemel and Lederer presented their quantitative results of 8-week-incubations of lysozyme and glucose in the presence of OPD at 37 °C.²³ Further investigations are necessary in order to assess the importance of these dicarbonyl compounds in the overall Maillard processes.

3. Experimental

3.1. General methods

¹H NMR (500 MHz), ¹H, ¹H-COSY (correlation spectroscopy), ¹H, ¹H-TOCSY (total correlation spectroscopy), TOCSY 1D (one-dimensional), gs-HMBC (gradient-selected heteronuclear multiple bond correlation), and gs-HSQC (gradient-selected heteronuclear single quantum coherence) spectra were recorded at 25 °C on a Varian (Darmstadt, Germany) Unity Inova 500 spectrometer in D₂O. The LC-(ESI; electrospray

Table 2. ^1H and ^{13}C NMR spectroscopic data of **18** and **20**^a in D_2O

	18a	18b	20a	20b
^1H NMR	δ (ppm) ^b			
H ₂ -1	3.21		3.22	
H _A -1		3.16		3.11
H _B -1		3.42		3.25
H-2	3.98	3.94	3.99	3.94
H-3	4.17	4.11	4.24	4.14
H _A -4	3.10	3.08	3.25	3.13
H _B -4	3.25	3.28	3.37	3.59
H-7			5.30	5.35
H ₂ -7	4.95	4.94		
H _A -8			3.91	3.87
H _B -8			3.98	3.92
H ₂ -1'	3.06	3.06	3.07	3.04
H ₂ -2'	1.70	1.70	1.70	1.70
H ₂ -3'	1.42	1.42	1.42	1.42
H ₂ -4'	1.80	1.80	1.81	1.81
H-5'	3.67	3.68	3.67	3.67
H-3''	7.90	7.90	7.98	7.98
H-4''	7.74	7.74	7.79	7.79
H-5''	7.74	7.74	7.79	7.79
H-6''	7.94	7.94	8.04	8.04
	J (Hz) ^c			
$^2J_{1\text{A},1\text{B}}$		(-)13.0		(-)13.0
$^2J_{4\text{A},4\text{B}}$	(-)15.0	(-)15.0	(-)15.0	(-)15.0
$^2J_{8\text{A},8\text{B}}$			(-)12.0	(-)12.0
$^3J_{1,2}$	6.5		6.9	
$^3J_{1\text{A},2}$		9.7		3.5
$^3J_{1\text{B},2}$		3.0		2.5
$^3J_{2,3}$	2.7	6.6	2.7	3.3
$^3J_{3,4\text{A}}$	3.9	10.1	4.6	10.2
$^3J_{3,4\text{B}}$	9.5	3.3	9.6	3.0
$^3J_{7,8\text{A}}$			4.5	6.0
$^3J_{7,8\text{B}}$			6.3	1.8
$^3J_{1',2'}$	7.6	7.6	8.4	8.6
$^3J_{4',5'}$	6.1	6.1	6.0	6.0
^{13}C NMR	δ (ppm) ^b			
C-1	50.3	49.7	50.2	48.8
C-2	69.0	70.3	69.1	69.1
C-3	71.6	72.8	71.7	71.7
C-4	37.2	37.2	37.5	37.5
C-5	154.0	154.0	155.0	155.0
C-6	154.0	154.0	155.5	155.5
C-7	62.8	62.8	71.0	71.0
C-8			65.1	65.1
C-1'	47.8	47.8	47.8	47.8
C-2'	25.3	25.3	25.2	25.2
C-3'	22.1	22.1	22.1	22.1
C-4'	30.2	30.2	30.2	30.2
C-5'	54.8	54.8	54.7	54.7
C-6'	175.4	175.4	176.0	176.0

(continued on next page)

Table 2 (continued)

	18a	18b	20a	20b
C-1''	141.0	141.0	141.0	141.0
C-2''	140.0	140.0	140.0	140.0
C-3''	128.1	128.1	128.1	128.1
C-4''	131.2	131.2	131.3	131.3
C-5''	131.2	131.2	131.3	131.3
C-6''	128.7	128.7	128.7	128.7

Hydrogen/carbon assignment has been validated by ^1H , ^1H -COSY, TOCSY 1D, gs-HSQC, and gs-HMBC measurements.

^aThe arrows in the structural formulas indicate the characteristic carbon–proton long-range coupling connectivities from the gs-HMBC spectra.

^b δ (ppm), chemical shift for the indicated hydrogen/carbon.

^c J (Hz), coupling constant between the indicated protons.

ionization) MS analyses were run on an HP1100 (Hewlett-Packard, Waldbronn, Germany) high-performance liquid chromatography (HPLC) system coupled to a Micromass (Manchester, UK) VG platform II quadrupole mass spectrometer equipped with an ESI interface. The HPLC system comprised an HP1100 autosampler, HP1100 gradient pump, HP1100 thermostat, and HP1100 diode array detector (DAD) module. Column: 150 mm \times 4.6 mm i.d., 5 μm , YMC-Pack Pro C18; 10 mm \times 4.6 mm i.d. guard column (YMC Europe, Schermbeck, Germany); column temperature, 25 $^\circ\text{C}$; flow rate, 1.0 mL/min; injection volume, 20 μL . Gradients: 10 mM ammonium formate buffer (pH 4.0)–MeOH. (A) 5% MeOH, 0 min; 95% MeOH, 30–35 min; 5% MeOH, 40–45 min. (B) 5% MeOH, 0 min; 50% MeOH, 25 min; 95% MeOH, 30–35 min; 5% MeOH, 40–47 min. Post-column splitting ratio, 1:20. MS parameters: ESI⁺; source temperature, 120 $^\circ\text{C}$; capillary, 3.5 kV; HV lens, 0.5 kV; cone voltage, 55 V. The MS system was operated in the full scan mode (m/z 150–1000). For accurate mass determination, data were collected in the multichannel acquisition (MCA) mode with 128 channels per m/z unit using 12 scans (6 s) with 0.1 s reset time. The resolution was 1060–1110 (10% valley definition). The sample was dissolved in water/MeCN (1:1) containing reference material (0.1 $\mu\text{g}/\mu\text{L}$, see below), ammonium formate (0.1%), and formic acid (1%); the sample concentration was similar to that of the reference compound. The solution was introduced into the ESI source (80 $^\circ\text{C}$) at a flow rate of 5 $\mu\text{L}/\text{min}$. The following scan ranges and reference peaks were used for calibration: **12**, m/z 335–435; poly(ethylene glycol) 350 monomethyl ether, m/z 341.3275, 358.2440, 385.2437, 402.2703, 429.2699; **14a**, m/z 335–435; poly(ethylene glycol) 350 monomethyl ether, m/z 341.3275, 358.2440, 385.2437, 402.2703, 429.2699; **14b**, m/z 335–435; poly(ethylene glycol) 400, m/z 344.2284, 371.2281, 388.2546, 415.2543; **16**, m/z 250–360; poly(ethylene glycol) 350 monomethyl ether, m/z 253.1658, 270.1915, 297.1906, 314.2206, 341.2171, 358.2465; **18**, m/z 350–450; poly(ethylene glycol) 350 monomethyl ether, m/z 358.2470, 385.2415, 402.2789, 429.2689, 446.3003; **20**, m/z 380–460; poly(ethylene glycol) 350 monomethyl ether, m/z 385.2436, 402.2733, 429.2715, 446.2979,

473.2978. MassLynx 3.2 software was used for data acquisition and processing. The preparative HPLC system consisted of a Kronlab (Sinsheim, Germany) KD200/100SS gradient pump system combined with a Knauer (Berlin, Germany) A0293 variable wavelength detector and a 250 mm \times 20 mm i.d., 7 μm , Nucleosil C 18 column with 50 mm \times 20 mm i.d. guard column (Kronlab); injection volume, 1.5 mL; flow rate, 20 mL/min. Gradients were applied as follows: 10 mM ammonium formate buffer (pH 4.0)–MeOH. (A) 5% MeOH, 0 min; 70% MeOH, 20 min; 100% MeOH, 22–25 min; 5% MeOH, 28–33 min. (B) 5% MeOH, 0 min; 55% MeOH, 12 min; 100% MeOH, 15–18 min; 5% MeOH, 20–25 min.

3.2. Materials

Milli-Q water, purified to 18 M Ω /cm² (Millipore, Eschborn, Germany), was used in the preparation of all solutions. HPLC grade MeOH was employed for LC-MS. For preparative HPLC, solvents were degassed by flushing with helium. D-Erythrose, D-galactose, D-glucose-6-phosphate disodium salt dihydrate, D-glycero-D-mannoheptose, D-lactose, D-mannose, D-melibiose, *N* $^\alpha$ -*t*-Boc-L-lysine, and *o*-phenylenediamine (OPD) were purchased from Fluka (Neu-Ulm, Germany); poly(ethylene glycol) 400 and poly(ethylene glycol) 350 monomethyl ether were from Aldrich (Steinheim, Germany); diethylenetriaminepentaacetic acid (DTPA), D-glucose-L-talooctose, and D-gentiobiose were from Sigma (Steinheim, Germany). For a phosphate buffer salt mixture giving solutions with pH 7.4, KH₂PO₄ (2.68 g; 20 mmol) and Na₂HPO₄·2H₂O (14.3 g; 80 mmol) were mixed vigorously.

3.3. Incubations of hexoses and (1 \rightarrow 4) glycosidic linked disaccharides with lysine side chains in the presence of OPD

N $^\alpha$ -*t*-Boc-L-lysine (615 mg; 25 mmol), DTPA (10 mg; 25 μmol), OPD (107.5 mg; 1 mmol), and phosphate buffer, pH 7.4 (425 mg; 2.5 mmol), were dissolved in 25 mL of water. To 5 aliquots (5 mL each), D-glucose, D-mannose, D-galactose (90 mg; 0.5 mmol), D-lactose, and D-maltose (180 mg; 0.5 mmol) were added, filtered

(sterile filter 0.2 μm), flushed with argon, and kept at 60 °C. At regular intervals 100 μL were taken and the protective group was cleaved with 150 μL 3 M HCl at ambient temperature for 30 min. The hydrolyzates were diluted with water (250 μL), the pH adjusted to 7 by slowly adding solid NaHCO_3 , and analyzed by LC-(ESI)MS (gradient A). Retention times of the obtained quinoxalines with $[\text{M}+\text{H}]^+$ at m/z 363 from hexoses, t_R 8.3 min and from disaccharides, t_R 5.6 min.

3.4. N^6 -[3-(2,3-Dihydroxypropyl)quinoxalin-2-yl]-methyl]-L-lysine (**12**)

D-Lactose (720 mg; 2 mmol), N^α -*t*-Boc-L-lysine (1.48 g; 6 mmol), OPD (432 mg; 4 mmol), DTPA (4 mg; 0.01 mmol), and phosphate buffer, pH 7.4 (170 mg; 1 mmol), were dissolved in 10 mL of water. The mixture was flushed with argon, kept at 60 °C for 3 days, and purified by preparative HPLC (gradient A; detection wavelength, 318 nm). Fractions with t_R 19.9 min yielded, after lyophilization, crude N^2 -(*tert*-butoxycarbonyl)- N^6 -[3-(2,3-dihydroxypropyl)quinoxalin-2-yl]methyl]-L-lysine (*t*-Boc-**12**). LC-(ESI)MS (gradient A): t_R 17.2 min, m/z 463.2 $[\text{M}+\text{H}]^+$.

This product was dissolved in aqueous 3 M HCl (3 mL) and kept at room temperature for 30 min. The pH was adjusted to 7 by slowly adding solid NaHCO_3 , the volume finally filled up to 5 mL, and the mixture subjected to preparative HPLC (gradient B; detection wavelength, 318 nm). Fractions with t_R 5.6 min yielded, after lyophilization, **12** (46 mg; 0.13 mmol; 6.35%). LC-(ESI)MS (gradient A): **12**, t_R 5.6 min, m/z 363.2 $[\text{M}+\text{H}]^+$. Accurate mass (mean of eight measurements \pm SD): **12**, m/z 363.2028 \pm 0.0008 $[\text{M}+\text{H}]^+$ (363.2032, calcd for $\text{C}_{18}\text{H}_{27}\text{N}_4\text{O}_4$). For NMR data, see Table 1.

3.5. N^6 -[2,3-Dihydroxy-3-(3-methylquinoxalin-2-yl)propyl]-L-lysine (**14**)

D-Glucose-6-phosphate-2H₂O (680.3 mg; 2 mmol), N^α -*t*-Boc-L-lysine (1.48 g; 6 mmol), OPD (432 mg; 4 mmol), DTPA (4 mg; 0.01 mmol), and phosphate buffer, pH 7.4 (170 mg; 1 mmol), were dissolved in 10 mL of water. The mixture was flushed with argon, kept at 60 °C for 3 days, and purified by preparative HPLC (gradient A; detection wavelength, 318 nm). Fractions with t_R 20.8 min yielded, after lyophilization, N^2 -(*tert*-butoxycarbonyl)- N^6 -[2,3-dihydroxy-3-(3-methylquinoxalin-2-yl)propyl]-L-lysine (*t*-Boc-**14**). LC-(ESI)MS (gradient A): diastereoisomer I, t_R 17.8 min, m/z 463.2 $[\text{M}+\text{H}]^+$; diastereoisomer II, t_R 18.2 min, m/z 463.2 $[\text{M}+\text{H}]^+$.

This crude compound was dissolved in aqueous 3 M HCl (3 mL) and kept at ambient temperature for 30 min. The pH was adjusted to 7 by slowly adding solid NaHCO_3 , the volume finally filled up to 5 mL, and

purified by preparative HPLC (gradient B; detection wavelength, 318 nm). Fractions with t_R 10.1 min and t_R 10.4 min yielded, after lyophilization, **14a** (10.0 mg; 0.028 mmol; 1.38%) and **14b** (20.1 mg; 0.055 mmol; 2.77%), respectively. LC-(ESI)MS (gradient A): **14a**, t_R 7.1 min, m/z 363.2 $[\text{M}+\text{H}]^+$; **14b**, t_R 7.5 min, m/z 363.2 $[\text{M}+\text{H}]^+$. Accurate mass (mean of 10 measurements \pm SD): **14a**, m/z 363.2033 \pm 0.0017 $[\text{M}+\text{H}]^+$; **14b**, m/z 363.2034 \pm 0.0011 $[\text{M}+\text{H}]^+$ (363.2032, calcd for $\text{C}_{18}\text{H}_{27}\text{N}_4\text{O}_4$). For NMR data, see Table 1.

3.6. Formation of **14** from D-melibiose and D-gentiobiose

D-Melibiose (36 mg; 0.1 mmol) and D-gentiobiose (34.2 mg; 0.1 mmol) were incubated with N^α -*t*-Boc-L-lysine (74 mg; 0.3 mmol), OPD (21.6 mg; 0.2 mmol), DTPA (0.2 mg; 0.5 μmol), and phosphate buffer, pH 7.4 (8.5 mg; 0.05 mmol), in water (0.5 mL) at 60 °C for 3 days, respectively. LC-(ESI)MS analysis (gradient A) showed two signals for *t*-Boc-**14**, t_R 17.8 min and t_R 18.2 min, m/z 463.2 $[\text{M}+\text{H}]^+$, respectively, and the characteristic UV spectra for quinoxalines.

3.7. N^6 -[3-(3-Methylquinoxalin-2-yl)methyl]-L-lysine (**16**)

D-Erythrose (144 mg; 1.2 mmol), N^α -*t*-Boc-L-lysine (886.8 mg; 3.6 mmol), OPD (259.2 mg; 2.4 mmol), DTPA (2.4 mg; 0.006 mmol), and phosphate buffer, pH 7.4 (102 mg; 0.6 mmol), were dissolved in 6 mL of water. The mixture was flushed with argon, kept at 70 °C for 24 h, and purified by preparative HPLC (gradient A; detection wavelength, 318 nm). Fractions with t_R 21.1 min yielded, after lyophilization, crude N^2 -(*tert*-butoxycarbonyl)- N^6 -[3-(3-methylquinoxalin-2-yl)methyl]-L-lysine (*t*-Boc-**16**). LC-(ESI)MS (gradient A): t_R 18.2 min, m/z 403.2 $[\text{M}+\text{H}]^+$.

This crude product was dissolved in aqueous 3 M HCl (2 mL) and kept at room temperature for 30 min. The pH was adjusted to 5 by slowly adding solid NaHCO_3 , the volume finally filled up to 5 mL, and the mixture subjected to preparative HPLC (gradient B; detection wavelength, 318 nm). Fractions with t_R 9.9 min yielded, after lyophilization, **16** (8.3 mg; 0.027 mmol; 2.28%). LC-(ESI)MS (gradient A): t_R 6.1 min, m/z 303.2 $[\text{M}+\text{H}]^+$. Accurate mass (mean of nine measurements \pm SD): **16**, m/z 303.1828 \pm 0.0007 $[\text{M}+\text{H}]^+$ (303.1821, calcd for $\text{C}_{16}\text{H}_{23}\text{N}_4\text{O}_2$). For NMR data, see Table 1.

3.8. N^6 -{2,3-Dihydroxy-4-[3-(hydroxymethyl)quinoxalin-2-yl]butyl]-L-lysine (**18**)

D-glycero-D-Mannoheptose (252 mg; 1.2 mmol), N^α -*t*-Boc-L-lysine (886.8 mg; 3.6 mmol), OPD (259.2 mg;

2.4 mmol), DTPA (2.4 mg; 0.006 mmol), and phosphate buffer, pH 7.4 (102 mg; 0.6 mmol), were dissolved in 6 mL of water. The mixture was flushed with argon, kept at 70 °C for 3 days, and purified by preparative HPLC (gradient A; detection wavelength, 318 nm). Fractions with t_R 20.0 min yielded, after lyophilization, crude N^2 -(*tert*-butoxycarbonyl)- N^6 -{2,3-dihydroxy-4-[3-(hydroxymethyl)quinoxalin-2-yl]butyl}-L-lysine (*t*-Boc-**18**). LC-(ESI)MS (gradient A): t_R 17.5 min, m/z 493.2 $[M+H]^+$.

This compound was dissolved in aqueous 3 M HCl (2 mL) and kept at ambient temperature for 30 min. The pH was adjusted to 5 by slowly adding solid $NaHCO_3$, the volume finally filled up to 5 mL, and finally purified by preparative HPLC (gradient B; detection wavelength, 318 nm). Fractions with t_R 11.0 min yielded, after lyophilization, **18** (3 mg; 0.008 mmol; 0.64%). LC-(ESI)MS (gradient A): **18a**, t_R 7.4 min, m/z 393.2 $[M+H]^+$; **18b**, t_R 7.5 min, m/z 393.2 $[M+H]^+$. Accurate mass (mean of 10 measurements \pm SD): **18**, m/z 393.2139 \pm 0.0004 $[M+H]^+$ (393.2138, calcd for $C_{19}H_{29}N_4O_5$). For NMR data, see Table 2.

3.9. N^6 -{4-[3-(1,2-Dihydroxyethyl)quinoxalin-2-yl]-2,3-dihydroxybutyl}-L-lysine (**20**)

D-glucose-L-Talooctose (240 mg; 1 mmol), N^2 -*t*-Boc-L-lysine (739 mg; 3 mmol), OPD (216 mg; 2 mmol), DTPA (2 mg; 0.005 mmol), and phosphate buffer, pH 7.4 (84.5 mg; 0.5 mmol), were dissolved in 5 mL of water. The mixture was flushed with argon, kept at 70 °C for 3 days, and purified by preparative HPLC (gradient A; detection wavelength, 318 nm). Fractions with t_R 19.5 min yielded, after lyophilization, crude N^2 -(*tert*-butoxycarbonyl)- N^6 -{4-[3-(1,2-dihydroxyethyl)quinoxalin-2-yl]-2,3-dihydroxybutyl}-L-lysine (*t*-Boc-**20**). LC-(ESI)MS (gradient A): t_R 16.9 min, m/z 523.2 $[M+H]^+$.

This product was dissolved in aqueous 3 M HCl (2 mL) and kept at room temperature for 30 min. The pH was adjusted to 5 by slowly adding solid $NaHCO_3$, the volume finally filled up to 5 mL, and the mixture subjected to preparative HPLC (gradient B; detection wavelength, 318 nm). Fractions with t_R 10.6 min yielded, after lyophilization, **20** (9.5 mg; 0.02 mmol; 2.25%). LC-(ESI)MS (gradient A): **20a**, t_R 7.1 min, m/z 423.2 $[M+H]^+$; **20b**, t_R 7.2 min, m/z 423.2 $[M+H]^+$. Accurate mass (mean of seven measurements \pm SD): **20**, m/z 423.2232 \pm 0.0012 $[M+H]^+$ (423.2244, calcd for $C_{20}H_{31}N_4O_6$). For NMR data, see Table 2.

Acknowledgements

We are grateful to Dr. J. Conrad and S. Mika, Institute of Chemistry, University of Hohenheim, for recording the NMR spectra. We thank Dr. K. M. Biemel, Re-

gional Veterinary and Food Control Agency Stuttgart, for many helpful discussions.

References

- Ledl, F.; Schleicher, E. *Angew. Chem., Int. Ed. Engl.* **1990**, *29*, 565–706.
- Friedman, M. J. *J. Agric. Food Chem.* **1996**, *44*, 631–653.
- Biemel, K. M.; Reihl, O.; Conrad, J.; Lederer, M. O. *J. Biol. Chem.* **2001**, *276*, 23405–23412.
- Shin, D. B.; Hayase, F.; Kato, H. *Agric. Biol. Chem.* **1988**, *52*, 1451–1458.
- Glomb, M. A.; Pfahler, C. *Carbohydr. Res.* **2000**, *329*, 515–523.
- Vasan, S.; Zhang, X.; Kapurniotu, A.; Bernhagen, J.; Teichberg, S.; Basgen, J.; Wagle, D.; Shih, D.; Terlecky, I.; Bucala, R.; Cerami, A.; Egan, J.; Ulrich, P. *Nature* **1996**, *382*, 275–278.
- Nagaraj, R. H.; Shipanova, I. N.; Faust, F. M. *J. Biol. Chem.* **1996**, *271*, 19338–19345.
- Lederer, M. O.; Klaiber, R. G. *Bioorg. Med. Chem.* **1999**, *7*, 2499–2507.
- Odani, H.; Shinzato, T.; Usami, J.; Matsumoto, Y.; Brinkmann-Frye, E.; Baynes, J. W.; Maeda, K. *FEBS Lett.* **1998**, *427*, 381–385.
- Biemel, K. M.; Conrad, J.; Lederer, M. O. *Angew. Chem., Int. Ed.* **2002**, *41*, 801–804.
- Monnier, V. M.; Kohn, R. R.; Cerami, A. *Proc. Natl. Acad. Sci. U.S.A.* **1984**, *81*, 583–587.
- Schmidt, A. M.; Hori, O.; Brett, J.; Yan, S. D.; Wautier, J. L.; Stern, D. *Arterioscler. Thromb.* **1994**, *14*, 1521–1528.
- Kislinger, T.; Fu, C. F.; Huber, B.; Qu, W.; Taguchi, A.; Yan, S. D.; Hofmann, M.; Yan, S. F.; Pischetsrieder, M.; Stern, D.; Schmidt, A. M. *J. Biol. Chem.* **1999**, *274*, 31740–31749.
- Schmidt, A. M.; Yan, S. D.; Yan, S. F.; Stern, D. M. *Biochem. Biophys. Acta* **2000**, *1498*, 99–111.
- Baynes, J. W.; Thorpe, S. R. *Diabetes* **1999**, *48*, 1–9.
- Colaco, C. A. L. S. *The Glycation Hypothesis of Atherosclerosis*; Springer: Heidelberg, 1997.
- Yan, S. D.; Chen, J.; Fu, J.; Chen, M.; Zhu, H.; Roher, A.; Slattery, T.; Zhao, L.; Nagashima, M.; Morser, J.; Migheli, A.; Nawroth, P.; Stern, D.; Schmidt, A. M. *Nature* **1996**, *382*, 685–691.
- Takeda, A.; Yasuda, T.; Miyata, T.; Goto, Y.; Wakai, M.; Watanabe, M.; Yasuda, Y.; Horie, K.; Inagaki, T.; Doyu, M.; Maeda, K.; Sobue, G. *Acta Neuropathol.* **1998**, *95*, 555–558.
- Biemel, K. M.; Lederer, M. O. *Bioconj. Chem.* **2003**, *14*, 619–628.
- Glomb, M. A.; Tschirnich, R. *J. Agric. Food Chem.* **2001**, *49*, 5534–5550.
- Ulrich, P.; Cerami, A. *Recent Prog. Horm. Res.* **2001**, *56*, 1–21.
- Vlassara, H.; Striker, L. J.; Teichberg, S.; Fu, H.; Li, Y. M.; Steffes, M. *Proc. Natl. Acad. Sci. U.S.A.* **1994**, *91*, 11704–11708.
- Biemel, K. M.; Lederer, M. O. *Bioconj. Chem.* **2003**, *14*, 619–628.
- Huber, B.; Ledl, F. *Carbohydr. Res.* **1990**, *204*, 215–220.
- Feather, M. S.; Mossine, V. V. *The Royal Soc. Chem.* **1998**, *223*, 37–42.
- Mossine, V. V.; Glinsky, G. V.; Feather, M. S. *Carbohydr. Res.* **1994**, *262*, 257–270.